Draft version November 23, 2016
Typeset using LaTeX **twocolumn** style in AASTeX61

FRB 121102: MULTI-TELESCOPE BURST PROPERTIES AND IMPLICATIONS FOR FRB POPULATION

C. J. Law,[1] R. S. Wharton,[2] M. A. McLaughlin,[3,4] J. M. Cordes,[2] G. C. Bower,[5] S. Burke-Spolaor,[6,3,4] B. J. Butler,[6] S. Chatterjee,[2] P. Demorest,[6] J. W. T. Hessels,[7,8] R. Fender,[9] T. J. W. Lazio,[10] K. Mooley,[9] M. Rupen,[11] L. G. Spitler,[12] P. Scholz,[11] and A. Seymour[13,14]

[1] *Dept of Astronomy and Radio Astronomy Lab, University of California, Berkeley, CA 94720, USA*
[2] *Cornell Center for Astrophysics and Planetary Science and Department of Astronomy, Cornell University, Ithaca, NY 14853, USA*
[3] *Department of Physics and Astronomy, West Virginia University, Morgantown, WV 26506, USA*
[4] *Center for Gravitational Waves and Cosmology, West Virginia University, Chestnut Ridge Research Building, Morgantown, WV 26505*
[5] *Academia Sinica Institute of Astronomy and Astrophysics, 645 N. A'ohoku Place, Hilo, HI 96720, USA*
[6] *National Radio Astronomy Observatory, Socorro, NM 87801, USA*
[7] *ASTRON, Netherlands Institute for Radio Astronomy, Postbus 2, 7990 AA, Dwingeloo, The Netherlands*
[8] *Anton Pannekoek Institute for Astronomy, University of Amsterdam, Science Park 904, 1098 XH Amsterdam, The Netherlands*
[9] *University of Oxford, UK*
[10] *Jet Propulsion Laboratory, California Institute of Technology, Pasadena, CA 91109, USA*
[11] *National Research Council of Canada, Herzberg Astronomy and Astrophysics, Dominion Radio Astrophysical Observatory, P.O. Box 248, Penticton, BC V2A 6J9, Canada*
[12] *Max-Planck-Institut für Radioastronomie, Auf dem Hügel 69, D-53121 Bonn, Germany*
[13] *Arecibo Observatory, HC3 Box 53995, Arecibo, PR 00612, USA*
[14] *Max-Planck-Institut für Radioastronomie, Auf dem Hügel 69, Bonn, D-53121, Germany*

ABSTRACT

The millisecond radio transients known as Fast Radio Bursts have recently emerged as a mysterious, new class of astrophysical transient. The discovery of repeating bursts from FRB 121102 has shown that at least some FRBs are not cataclysmic and opened potential for studying FRB properties via a homogenous sample of bursts. The recent localization of FRB 121102 with the Very Large Array has helped measure its distance and a host of intrinsic properties. This localization was made with 9 bursts seen by the VLA in coordination the Arecibo, Effelsberg, and AMI-LA observatories. We present a detailed analysis of these bursts, including the first simultaneous detection of an FRB with multiple telescopes. We show that the burst spectra typically have a broad Gaussian shape on the scale of ~ 500 MHz with fine spectral structure consistent with either scintillation or unresolved temporal structure. We present the luminosity distribution and temporal statistics for FRB 121102 and argue that the whole FRB population is adequately described by a single class similar to FRB 121102. We close with thoughts on optimal strategies to make new interferometric localizations of FRBs.

1. INTRODUCTION

Fast Radio Bursts (FRBs) are a new class of millisecond-duration radio transient with a dispersion measure (DM) that implies that they originate outside of our Galaxy. At extragalactic (and potentially cosmological) distances, they are not only unusually luminous, but they provide a new tracer of other galaxies and the intergalactic medium (IGM). In this way, FRBs have opened a whole new playground in astrophysics (e.g., Falcke & Rezzolla 2014; McQuinn 2014; Cordes & Wasserman 2016). However, that potential has been hamstrung by the lack of a definitive association of an FRB to an extragalactic host.

This paper is part of a series that presents the first localization and host identification of an FRB (CITE, CITE, ...). FRB 121102, also known as the "repeating FRB", was first detected in November 2012 by the Arecibo Observatory (Spitler et al. 2014). In mid 2015, new Arecibo observations revealed a series of bursts at the same DM and sky position demonstrating that FRBs are capable of repetition (Spitler et al. 2016). Beginning in August of 2015, we made the first of nine detections of FRB 121102 with the Very Large Array (CITE) and localized it with a precision of $0.1''$. Deep radio and optical observing shows that FRB 121102 is unambiguously associated with a persistent radio and optical source at a redshift of 0.193 (CITE).

FRB 121102 has now been localized three orders of magnitude better than any other FRB and placed at a cosmological distance. Its lookback and luminosity distances are 746 and 972 Mpc (**?**), which are orders of magnitude larger than any other millisecond transient. This shows that FRBs:

- are extremely luminous,
- have a significant DM contribution from the IGM, and
- can be used to probe the IGM and their host galaxy.

The promise implied by the first reported FRB (Lorimer et al. 2007) is now being realized.

The cosmological distance for FRB 121102 could have wide-ranging implications for the FRB population as a whole. However, it has not been demonstrated that FRB 121102 is representative of the overall FRB population. In fact, the repetition of its bursts is unique among all FRBs (Petroff et al. 2015), so it is natural to ask whether FRB 121102 is representative. An important first step is to demonstrate that the properties of FRB 121102 are consistent with the significant body of facts for the overall population (Macquart & Johnston 2015; Katz 2016). The repeating nature of FRB 121102 provides us with several statistical tests we can use to test this connection.

We can also assume that FRB 121102 is representative and use it to constrain the physical processes at play in the overall FRB population. Although we now know that FRBs are luminous, it is not yet clear what process generates the radio bursts themselves (Katz 2014; Luan & Goldreich 2014; Cordes & Wasserman 2016). The simultaneous FRB 121102 observing campaign with the VLA, Arecibo, Effelsberg, GBT, and AMI-LA gives a more complete picture of the spectral structure of FRB radio emission. FRB repetition also has strong implications for the number of FRB-generating systems in the universe (Connor et al. 2016).

Given that FRBs are now known to be useful probes of the IGM, there is strong justification for continuing searches for new detections and localizations. The relatively faint counterpart to FRB 121102 argues that direct localization of the radio burst will continue to be the best way to find optical hosts to measure distances. Our multi-telescope constraints on burst spectra, measurement of host properties, burst rate estimates, and other properties will inform new strategies for finding FRBs...

2. OBSERVATIONS

The data presented here were obtained from multiple programs and telescopes, but the central goal was to interferometrically localize FRB 121102 with the VLA. The observing strategy was to ensure simultaneous observing between the VLA and Arecibo observatories and add other observatories added on a best-effort basis. We coordinated observing between the VLA, Arecibo, Effelsberg, and AMI-LA telescopes, as shown in figure 1. Below, we summarize these observations, with a focus on those conducted simultaneous with VLA burst detections from FRB 121102.

2.1. *VLA*

The FRB 121102 observing campaign started in late 2015 with a 10 hr campaign observed at 1.4 GHz in the compact D configuration. In April through May 2016, we conducted a 40 hr campaign at 3 GHz in the C and CnB configurations in coordination with Arecibo. We concluded with a new, 40 hr, coordinated campaign from August through September 2016 in the B configuration and during the move to the most extended A configuration. In this last campaign, the first 34 hours of VLA observations were made at 3 GHz, while the last 6 hours were observed at 6 GHz. This paper focuses on the data collected at 3 GHz, which includes all burst detections.

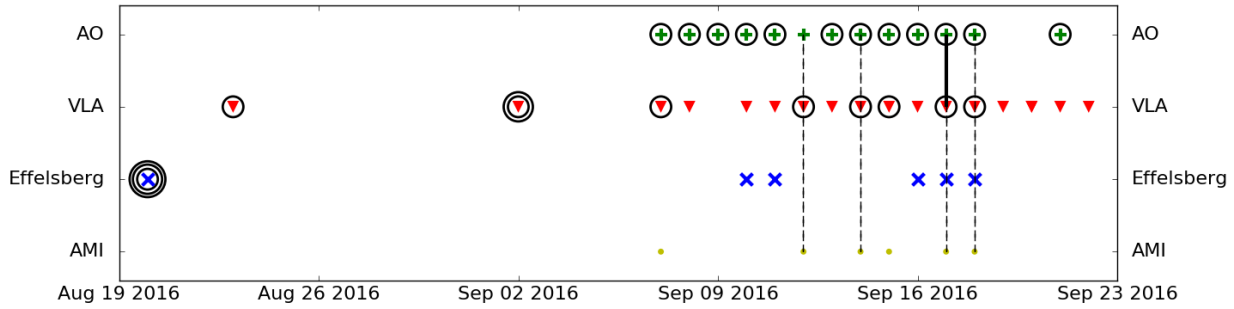

Figure 1. Summary of observing coverage and detections of FRB 121102 during the multi-telescope observing campaign. Symbols show days with observations and symbols with circles show detections of FRB 121102. Multiple circles indicate multiple burst detections, except for Arecibo, which typically has multiple detections per observing session (a detailed analysis is left for a future paper). The black dashed lines show the VLA burst detections with simultaneous coverage at other telescopes. The solid black line shows the simultaneous burst detection at VLA and Arecibo.

All VLA fast-sampled data were observed with 5 ms sampling, 256 channels, and dual-circular polarization (Law et al. 2015, as in). To maximize sensitivity, the channel frequency width was set to maintain sensitivity to the known DM of FRB 121102, while maximizing the total bandwidth. The total bandwidth at L (1.4 GHz), S (3 GHz), and C (6 GHz) bands was 256 MHz, 1024 MHz, and 2048 MHz, respectively. The 3 GHz data recorded data in 8 spectral windows with 32 channels each.

Observations in August and Septmeber were searched by a prototype version of *realfast*[1]. *realfast* is a real-time, fast imaging transient search system. The current, prototype runs on existing, CPU-based hardware of the VLA correlator backend, while the future *realfast* will run on a dedicated GPU cluster. The transient search pipeline software is called *rtpipe*[2] and is mostly written in Python. The transient search pipeline is described in Law et al. (2015) and performs data calibration, flagging, dedispersion, and imaging. Images were formed for each integration at DMs of 0, 546, 556.9, 560, and 565 pc cm^{-3}. Gain calibration is read from the "telcal" system, which uses phase-only calibration on the previous gain calibrator. A flux scale is calculated for each spectral window from an observation on *xx* and applied to all burst spectra.

Burst detections and localizations were made within hours of data being recorded. The transient search starts when data are recorded, but this prototype of *realfast* is a factor of several times slower than real-time, so we refer to the detection as "quasi real-time". Each image with a pixel higher than 6.4σ has some rudimentary data saved to capture both real and thermal-noise candidates as a check of data quality. For each image with a pixel higher than 7.4σ, *realfast* generates a candidate visualization with an image and spectrum. More detailed analysis, including improved calibration and localization, is conducted offline.

Computational notebooks to reproduce the transient detection and localization can be found at `https://github.com/caseyjlaw/FRB121102`. Time cut-out visibility data are available at `https://doi.org/10.7910/DVN/TLDKXG`. Original visibility data are available under VLA program codes 16A-459 and 16A-496 and can be downloaded at `http://archive.nrao.edu`.

2.2. *Arecibo*

During the joint Arecibo-VLA campaign, Arecibo observed with the L-wide receiver, which has an observational frequency range of 1.15 to 1.73 GHz and a full width at half maximum beam size of 3.3 arcmin. The PUPPI pulsar backend was used to record total intensity spectra with time and frequency resolutions of 10.24 μs and 1.5625 MHz, respectively, and full Stokes polarization information. Each frequency channel was coherently dedispersed to 557 pc cm^{-3}, thereby eliminating intra-channel dispersion smearing. PUPPI covers a total of 800 MHz of bandwidth centred at 1380.78125 MHz, but only $\sim$ 620 MHz of this band is usable due to radio frequency interference and receiver sensitivity roll-off at the band edges.

In total, twelve Arecibo observations had some simultaneous coverage with the VLA. Four of those observations were simultaneous with bursts detected with the VLA and one of those observations detected the same VLA burst. During the first VLA burst with Arecibo coverage (MJD 57643), the PUPPI system failed so data were recorded with xx (Jason?) at C band. No detection was made in that Arecibo data. Overall, there were

[1] See `http://realfast.io`.
[2] See `https://github.com/caseyjlaw/rtpipe`

many more bursts detected at Arecibo and a more detailed analysis will be presented in a future paper.

2.3. *Effelsberg*

Observations were conducted at an observing frequency of 4.6 to 5.1 GHz. The S60mm receiver has a system equivalent flux density of 18 Jy and a full-width half-max (FWHM) beam size of 2.4′at 4.85 GHz. Pulsar search mode data were recorded with the PFFTS backend. Total intensity spectra were recorded with a time resolution of 65.5 μs and a bandwidth of 500 MHz divided into 128 frequency channels. Note, the inter-channel DM smearing time for 560 pc cm^{-3} is $\sim$0.2 msec at 4.6 GHz.

Five Effelsberg observations had some simultaneous coverage with the VLA, of which two were simultaneous with VLA bursts. Unfortunately, due to a configuration error, a 100 MHz bandwidth filter centered at 4.85 GHz was in place for both of these sessions. The sensitivity was about two times worse than the nominal value. No burst was detected in either observation.

2.4. *AMI*

Kunal to provide description of AMI-LA

Six AMI-LA observations had some simultaneous coverage with the VLA, of which four covered VLA bursts. The upper limit on burst flux density limits any significant "afterglow". Deep image sensitivity is limited by confusion and is approximately equal to the flux density observed by VLA (CITE). Details from Kunal

3. RESULTS

3.1. *Multi-Telescope Burst Spectrum*

As shown in Figure 1, only one burst from FRB 121102 was detected simultaneously at more than one observatory. The VLA burst on 57648 was detected at Arecibo with a significance of xxσ (Jason) The relative time delay between the VLA and Arecibo is xx (Jason) ms...

Figure **to do** shows the dynamic spectrum formed from the phased VLA and Arecibo data... This simultaneous detection of a burst from roughly 1 to 4 GHz shows that some bursts cover more than an octave of frequency. This is one of three bursts with similar spectral coverage at Arecibo, so the other nondetections imply that those bursts had a smaller spectral coverage. In fact, as described in §3.2.1, most of the VLA bursts appear to be fully contained in the band from 2.5 to 3.5 GHz, which implies a much smaller spectral coverage for typical bursts.

Insert figure of VLA/AO dynamic spectrum on 57648

3.2. *VLA Bursts*

3.2.1. *Dynamic Spectra*

Figure 2 shows the spectrograms of all nine bursts detected by the VLA. We improved on the initial analysis presented in (CITE) by using a better calibration scheme and optimizing the image SNR over a fine DM grid. Table 1 shows the improved burst parameters using this new scheme.

The optimal DM values range from 552 to 572 pc cm^{-3} for all bursts and from 552 to 561 pc cm^{-3} for bursts with SNR$>$ 30. The expectation is that the VLA 3 GHz observing band will lose 10% of its sensitivity for DM in error by roughly 10 pc cm^{-3} (Cordes & McLaughlin 2003). However, the peak DM can be determined with a much higher precision (scaling linearly with the significance of the burst). We tested this model by simulating a burst with SNR= 30 and measuring its detection significance as a function of DM. The simulation parameters were reproduced at the known DM with a precision of roughly 1 pc cm^{-3}. This suggests that the measured variation in DM for FRB 121102is intrinsic to the bursts, rather than due to measurement uncertainty. This is consistent with the observation of intrinsic burst spectrotemporal structure that varies between bursts (CITE: WEIRD BURST).

3.2.2. *Spectral modeling*

After finding an optimal burst DM, we extract a spectrum from the integration with peak SNR. **need to confirm that bursts were unresolved in time**

Burst spectra are shown in Figure 3...

We fit a Gaussian model to each burst to estimate their characteristic width and peak flux... As shown in Table 1, the typical frequency scale is xx MHz...

3.2.3. *Spectral Autocorrelation*

The spectral autocorrelation is used to infer both intrinsic and scintillation properties (). Figure 4 shows the spectral autocorrellation for the MJD 57633.68 burst. Some marginal evidence of spectral correlation on the scale of the channel resolution (4 MHz)?

3.2.4. *Circular Polarization*

The VLA S-band recievers natively measure circular polarization, although observations did not include polarization calibration procedures. Crude constraints on circular polarization are possible by comparing the burst intensity in right and left-hand polarized data products. The apparent circular polarization fraction $((RR-LL)/(RR+LL))$ for the most significant bursts are all less than 3%. FRB121102 was located 2.3 arcmin away from pointing center, where systematic effects have

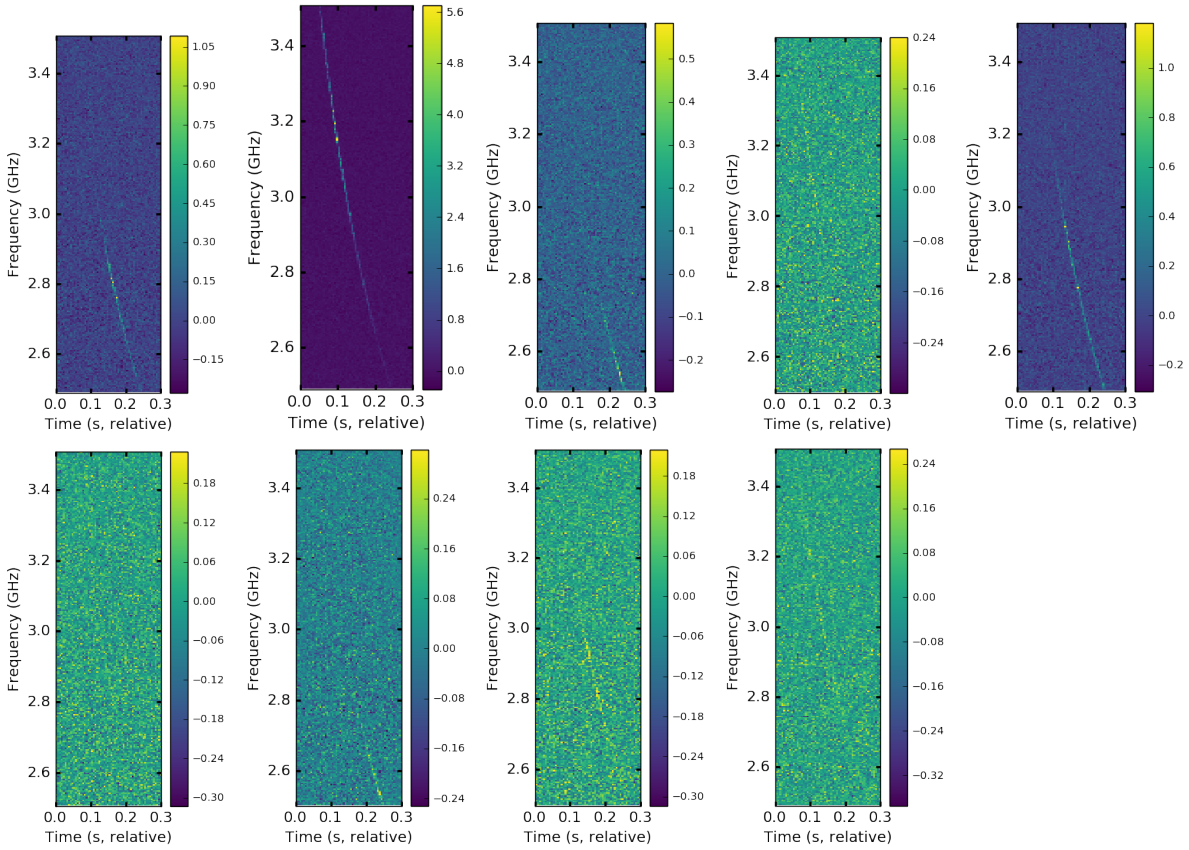

Figure 2. Spectrograms (time vs frequency intensity maps) for the nine VLA bursts. Starting at the top left, the correspond to bursts 57623, 57633.68, 57633.70, 57638, 57643, 57645, 57646, 57648, and 57649. Note that bursts are detected in 5 ms images generated from dedispersed visibilities.

been measured as large as 3% (Perley et al 2016, VLA memo). We conclude that the S-band bursts seen by the VLA have a circular polarization of less than 3%.

3.3. *Brightness Distribution*

The bursts seen by the VLA range in significance from 10 to 150σ. Table 1 shows the estimated burst luminosity from spectral modeling...

Figure 5 shows the flux distribution of the nine VLA bursts. Quantify flatness...

Compare luminosity distribution to flux distribution measured by (Vedantham et al. 2016)...

3.4. *Temporal Statistics*

Burst detections were made very inhomogenously though the roughly 63 hours of observing toward FRB 121102. Data quality are relatively high and RFI did not significantly impact sensitivity, so the inhomogeneous burst distribution not an observational artifact.

In the first ~ 25 hours observing at S-band no bursts were detected, while nine bursts were detected in the last $\sim$ 30 hours of S-band observing. Assuming the burst detection probability follows a stationary Poisson distribution, the nondetection in the first half of S-band limits the FRB rate to R < 0.12 hour^{-1}. The mean detection rate for the last part of the campaign was R $= 0.3$ hour^{-1}. The inconsistency shows that the detection probability is not stationary.

Moreover, there is weak evidence that the FRB 121102 burst rate changes during the last part of the campaign. We modeled the event detection probability as a Poisson probability with a rate parameter that scales linearly with time as $R = a + b * (\mathrm{MJD} - 57623)$. We then calculated the probability of measuring the observed event rate as $\Pi P_i(R)$. Figure 6 shows the (a, b) parameter space with contours of 50, 90, and 95% confidence contours.

Figure 7 shows a Lomb-Scargle periodogram... Lots of excess power corresponding to periods shorter than 1 hour.

4. DISCUSSION

4.1. *Luminosity Distribution*

Doubts were cast on the first FRB detection ("Lorimer burst") due to its unusually high brightness. The lack of lower-significance detections suggested that this burst

Table 1. Properties of Bursts from FRB 121102

Date (MJD)	S_{int} (mJy)	Image SNR	DM_{opt} (pc cm^{-3})	S_{peak} (mJy)	Center (GHz)	FWHM (MHz)
57623	258	38	561	0.41	2.8	300
57633.68	2000	179	554	1.90	3.2	520
57633.70	105	15	559	>0.188	<2.5	>350
57638	65	12	556	0.07	3.1	410
57643	375	100	560	0.39	2.8	520
57645	38	13	572	0.06	2.8	210
57646	69	20	555	>0.16	<2.5	>400
57648[a]	97	25	559	0.11	2.9	420
57649	110	36	552	0.07	2.9	880

[a]Detected simultaneously with Arecibo between 1.15 and 1.73 GHz.

was unlikely to be part of any astrophysical population. With more detections, it has become clear that the FRB population has a relatively flat flux distribution (Vedantham et al. 2016; Lawrence et al. 2016). This fact was demonstrated with yet another detection of an extremely bright FRB (Ravi et al. 2016).

Discuss comparison FRB 121102 luminosity distribution to that of FRB population... Imagine physical log N/log S with cut-offs and scattering can bias the intrinsic into the observed distribution (Macquart and Johnston)...

4.2. *Repetition*

Discussion of "red spectrum" and Connor et al. (2016). Bursts predict bursts therefore repetition constraints of other FRBs are likely weaker than claimed...

Constraints on repetition assuming "red spectrum" for whole population. Simulation using observed burst temporal statistics...

Intrinsic versus refractive scintillation...

Fewer FRBs out there...

4.3. *Emission Physics and Burst Energetics*

For a nominal Gpc distance D corresponding to redshifts $z \lesssim 0.3$, the received fluence A_ν from each burst implies a burst energy

$$E_{\rm burst} = 4\pi D^2 (\delta\Omega/4\pi) A_\nu \Delta\nu \approx 10^{38}\,{\rm erg}\,(\delta\Omega/4\pi) D^2_{\rm Gpc} (A_\nu/0.1\ {\rm Jy\,ms})(\Delta\nu/{\rm GHz}).$$

The unknown emission solid angle $\delta\Omega$ could be very small due to relativistic beaming, and together with a distance possibly much smaller than 1 Gpc, could reduce the energy requirement significantly. However, the *total* energy emitted could be larger depending on the duration of the emission in the source frame and other model-dependent details. Either way, the burst energies from FRB 121102 are not inconsistent with those that might be expected from the magnetosphere of a compact objectCordes & Wasserman (2016).

4.4. *Observing Strategies*

Repetition implies that targeting known FRBs is optimal.

Repetition and shallow luminosity distribution show that shallow and wide is the best way to blindly find FRBs.

Given that bursts have < 1 GHz-scale spectra, wide bandwidths improve odds of detection.

5. CONCLUSIONS

ACKNOWLEDGEMENTS

We thank ... This project was supported by the University of California Office of the President under Lab Fees Research Program Award 237863. The National Radio Astronomy Observatory is a facility of the National Science Foundation operated under cooperative agreement by Associated Universities, Inc.. This research made use of Astropy, a community-developed core Python package for Astronomy (Astropy Collaboration, 2013).

REFERENCES

Connor, L., Pen, U.-L., & Oppermann, N. 2016, MNRAS, 458, L89

Cordes, J. M., & McLaughlin, M. A. 2003, ApJ, 596, 1142

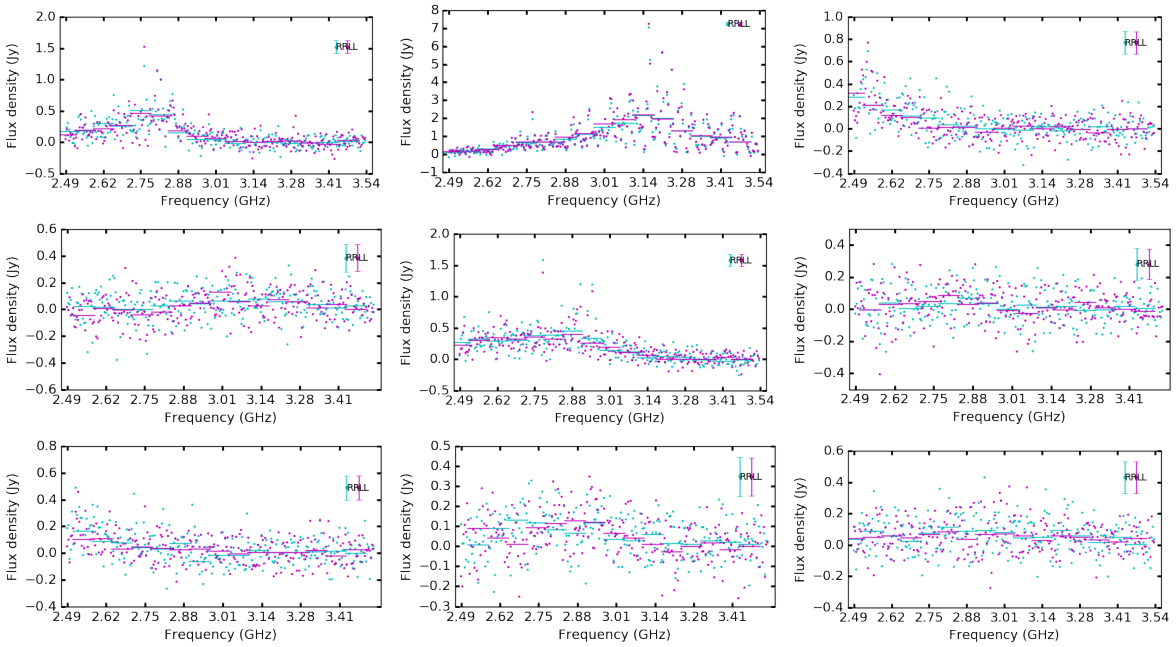

Figure 3. Spectra of nine bursts seen by the VLA from 2.5 to 3.5 GHz. Orthongonal circular polarizations (RR and LL) are plotted separately. **LABELS ALL SAME FREQ. SOME SHOULD START HIGHER FOR DROPPED CHANNELS**

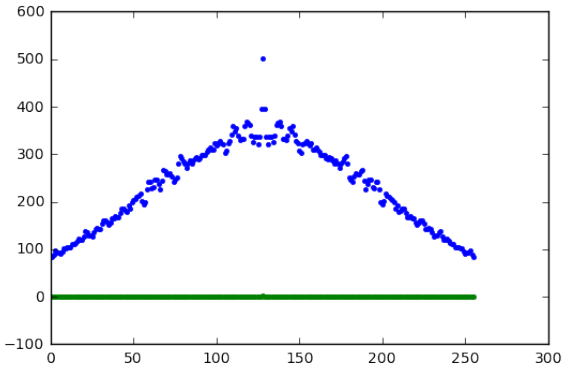

Figure 4.

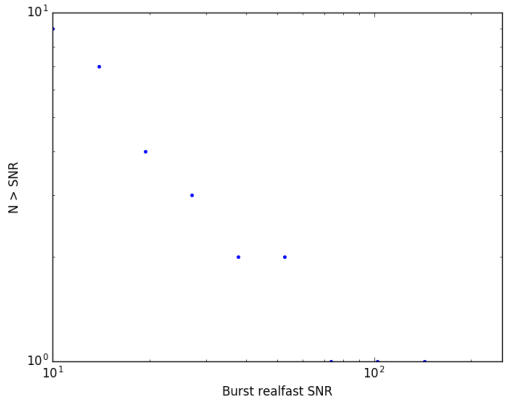

Figure 5. Log N – Log SNR distribution of real-time detections of FRB 121102. **Update to luminosity distribution**

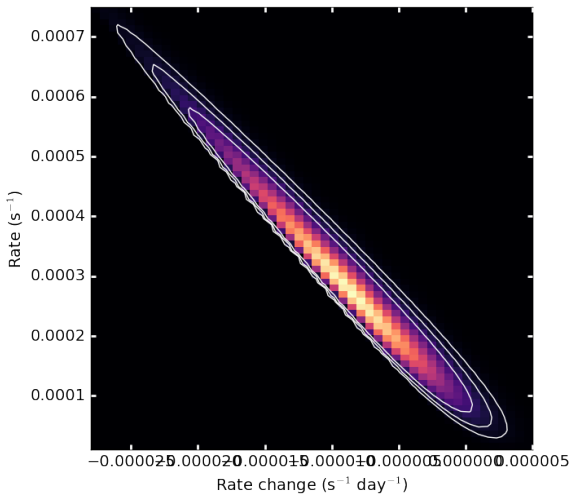

Figure 6. Rate versus rate change during last campaign.

Cordes, J. M., & Wasserman, I. 2016, MNRAS, 457, 232

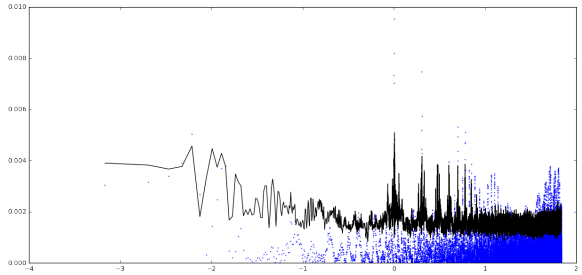

Figure 7. Lomb-Scargle periodogram with 95% limit on power from last observing campaign

Falcke, H., & Rezzolla, L. 2014, A&A, 562, A137

Katz, J. I. 2014, PhRvD, 89, 103009

—. 2016, Modern Physics Letters A, 31, 1630013

Law, C. J., et al. 2015, ApJ, 807, 16

Lawrence, E., Vander Wiel, S., Law, C. J., Burke Spolaor, S., & Bower, G. C. 2016, ArXiv e-prints

Lorimer, D. R., Bailes, M., McLaughlin, M. A., Narkevic, D. J., & Crawford, F. 2007, Science, 318, 777

Luan, J., & Goldreich, P. 2014, ApJL, 785, L26

Macquart, J.-P., & Johnston, S. 2015, MNRAS, 451, 3278

McQuinn, M. 2014, ApJL, 780, L33

Petroff, E., et al. 2015, MNRAS, 454, 457

Ravi, V., et al. 2016, ArXiv e-prints

Spitler, L. G., et al. 2014, ApJ, 790, 101

—. 2016, Nature, 531, 202

Vedantham, H. K., Ravi, V., Hallinan, G., & Shannon, R. M. 2016, ApJ, 830, 75